

Droplets sit and slide anisotropically on soft, stretched substrates

Katrina Smith-Mannschott,¹ Qin Xu,^{1,2} Stefanie Heyden,¹ Nicolas Bain,¹ Eric R. Dufresne,¹ and Robert W. Style¹

¹*Department of Materials, ETH Zürich, 8093 Zürich, Switzerland.*

²*Department of Physics, The Hong Kong University of Science and Technology, Hong Kong, China*

(Dated: July 9, 2022)

Anisotropically wetting substrates enable useful control of droplet behavior across a range of useful wetting applications. Usually, these involve chemically or physically patterning the substrate surface, or applying gradients in properties like temperature or electrical field. Here, we show that a flat, uniform, stretched, soft substrate also exhibits asymmetric wetting, both in terms of how droplets slide and in their static shape. Droplet dynamics are strongly affected by stretch: glycerol droplets on silicone substrates with a 23% stretch slide 70% faster in the direction parallel to the applied stretch than in the perpendicular direction. Contrary to classical wetting theory, static droplets in equilibrium take the shape of ellipsoids, oriented parallel to the stretch direction. Both effects arise from droplet-induced deformations of the substrate near the contact line.

While common surfaces have wetting responses that are direction-independent, nature has evolved a large variety of anisotropic surfaces that provide novel functionality. For example, desert beetles in arid climates use hydrophilic/hydrophobic patterns on their backs to collect dew [1], while spider webs perform a similar task with anisotropic fibres [2], and butterflies have anisotropically patterned wings that promote droplet run-off in certain directions [3].

Inspired by these natural phenomena, a variety of approaches to engineer anisotropic surfaces have been introduced [4]. Their applications include precise droplet control in microfluidics [5], novel surface coatings with unusual wetting properties [6], and water collection [7]. Such anisotropically-wetting surfaces can be made via a variety of methods. Surfaces can be chemically patterned with surface-energy gradients to drive droplets from high to low energy regions [8] or with stripes and other patterns to cause asymmetric spreading and pinning of droplets [9]. Similarly, micro-patterning surfaces with bumps, pillars, or various other features also drive the same phenomena [10–12].

All these surfaces involve significant efforts in fabrication. Alternatively, recent studies have shown that asymmetric wetting can be induced on free-standing thin elastic sheets through stretching [13, 14]. These membranes, with a thickness $\lesssim \mathcal{O}(1 \mu\text{m})$, are much thinner than the droplet radii. Droplet surface tension strongly deforms the sheet, whose thickness-integrated elastic stresses mimic anisotropic surface stresses [15]. As a result, static droplets acquire non-spherical shapes that reflect the underlying state of stress of the membrane.

Here we show that droplets anisotropically wet slabs of soft material that have been uniformly stretched, even when they are much smaller than the substrate thickness. Not only do droplets have non-spherical equilibrium shapes, but they also respond anisotropically to applied forces, sliding faster in one direction than another. These effects contradict the foundational theories of wetting, including Young’s Law. We show that they are governed by microscopic substrate deformations localized to the contact line (*e.g.* [16–18]) that respond

anisotropically to stretch.

We study the effect of strain on wetting behavior by investigating the behavior of glycerol droplets on soft, 1.0mm thick, silicone gels (CY52-276, Dow Corning) with a Young’s modulus of $E = 6\text{kPa}$. In equilibrium, on the unstretched substrate, these droplets have a macroscopic contact angle 95° [17]. We cut narrow strips from the substrate and uniaxially stretch these on a home-built stretching device. To ensure complete flatness, which we verify with interferometry in the Supplement, we placed sections of 1mm-diameter glass capillaries on the surface of the gel to suppress residual, longitudinal wrinkles (*c.f.* Figure 1). Strain, ϵ , was calculated either from imaging markings on the samples or from the displacement of the stretching device.

Droplets slide faster in the direction of applied stretch, as shown in Figure 1a. Here $5\mu\text{L}$ glycerol droplets slide along a vertical substrate with a uniaxial stretch of 23%, oriented either parallel (red) or perpendicular (purple) to gravity. This experiment was for 7-9 droplets in each orientation and the average trajectories are plotted in Figure 1b. Droplets sliding parallel to the stretch direction are 70% faster than those sliding perpendicular to the stretch direction. Interestingly, they also have clearly different shapes, with the faster droplets appearing to have a marked asymmetry between trailing and leading edges. Thus, moving millimetric droplets are sensitive to underlying stretch of soft materials.

The static shape of droplets is also sensitive to substrate deformation. Droplets tend to elongate in the direction of applied stretch, as shown in in Figure 2a,b. There images of two differently-sized droplets before and after $\epsilon = 50\%$ stretch are imaged with conventional brightfield and interference microscopy. In the unstretched case, droplets all remain completely circular, while in the stretched case, there is a small elongation along the stretch direction. While the effect is subtle in brightfield, there is a stark difference when the same droplets are imaged with an interferometric objective (bottom row), which shows changes to the substrate profile around the droplets. In the unstretched case, the interferometry fringes around the droplets are essentially

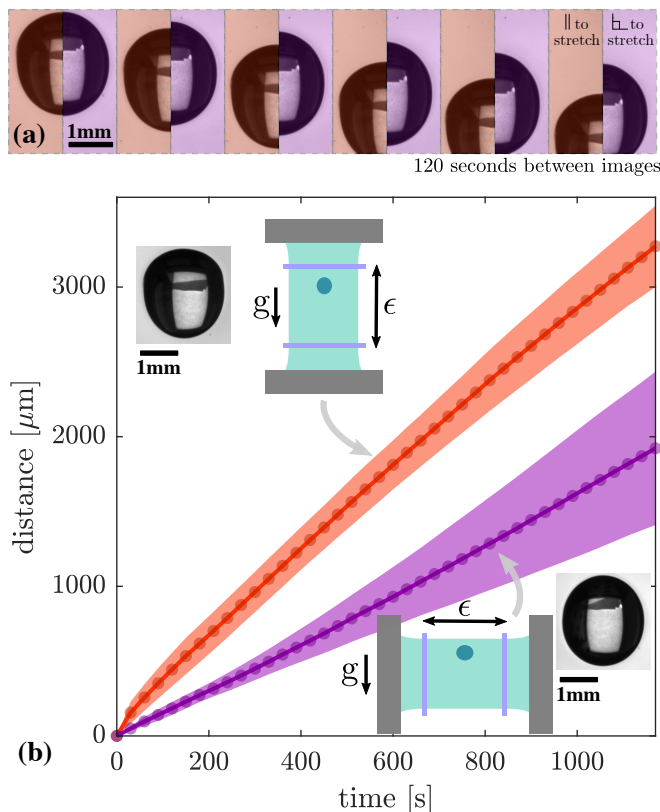


FIG. 1: Droplet dynamics depend on the underlying stretch. a) Droplets sliding parallel to the stretch (red) direction move faster than those sliding in the perpendicular (purple) direction and have clearly different shapes. b) Measured droplet positions vs time for sliding in the two different directions. This shows the average for 9 droplets sliding parallel to stretch and 7 droplets sliding perpendicular to stretch. $\epsilon = 23\%$. Shaded areas indicate one standard deviation to either side of the average.

symmetric and angle-independent (the top-left/bottom-right asymmetry results from a slight tilt of the substrate). However, in the stretched case, we see a strongly asymmetric, lobed pattern that extends perpendicular to the stretch direction.

Stretch-induced changes of shape could be a result of contact-line pinning or more subtle contact-angle hysteresis. Throughout this manuscript, for static equilibrium measurements, we minimize these possible effects by allowing droplets to equilibrate for at least one hour after deposition or stretching. Now, we completely rule out such hysteretic effects by comparing the final shape of droplets that are applied to the substrate before and after it is stretched, as shown in Figure 2c. We quantify droplet shape by plotting the difference between the long and short axis lengths of droplets, $l - w$, versus the average droplet radius, $(l + w)/2$, for over 1400 droplets. The shapes of droplets deposited before stretch (green) are identical to those deposited after stretch (yellow). This shows that there is essentially no hysteresis at these timescales on this substrate, in agreement with previ-

ous observations [19]. In both cases, the long axis of the droplet is always aligned with the the direction of stretch, as shown in the inset of Figure 2c.

This droplet-stretching behavior is limited to substrates with very low elastic moduli. We compare the shapes of droplets on the soft silicone with droplets on a 1.1mm-thick slab of much stiffer silicone ($E = 333\text{kPa}$, made following [20]), as shown in Figure 2d. While over 600 droplets on the soft substrate at $\epsilon = 20\%$, navy blue, show a pronounced increase of anisotropy with size, 345 droplets on the stiff substrate at a slightly larger strain of $\epsilon = 23\%$, purple, show no systematic variation in shape, with most of the recorded values of $l - w$ falling below the resolution of the imaging system. Indeed, the shapes of droplets on stretched stiff substrates are indistinguishable from those on unstretched, soft ones, shown in red. This is consistent with previous reports, which found no observable change to droplet shape when placed on stiffer substrates with different stretches [21].

These results suggest that the equilibrium shape of droplets on soft substrates depends on their size and the applied strain. To that end, we quantified the shapes of over 2150 droplets from 2 to 40 μm in radius over a range of uniaxial strains from 9-65%, as shown in Figure 2e. As seen previously, $l - w$ always increases monotonically with droplet size with the long axis of the droplet aligned with the stretch direction (see inset). For smaller droplets, the asymmetry, $(l - w)$, increases linearly with the droplet size. Equivalently, small droplets on the same applied stretch all have the same aspect ratio, l/w . At larger strains, the asymmetry increases more slowly with droplet size and the droplets become more circular (*i.e.* $l/w \rightarrow 1$). This trend is identical for all non-zero strains, as highlighted in Figure 2f. There each data set is normalized by the slope, α of the small-droplet data (radius $< 20\mu\text{m}$). Not only does this collapse the data onto a single curve for the small droplets, as it must, but it also collapses the transition to sublinear behavior for large droplets. This suggests a shift in the underlying physics occurring at a characteristic lengthscale around 30 μm . Note that scale factor α is not simply proportional to the applied strain, ϵ (see the inset). Thus the droplet reponse is not linear, and scaling the asymmetry by the applied strain, as in [22], is insufficient to collapse the data.

In the above results, we focused our analysis on the shape of droplet footprints. As these are non-circular, they suggest that the droplet itself should be aspherical. We confirm this using white-light profilometry, a technique which accurately measures the top of the droplet and the surface outside the contact line. This technique fails when the surface slope is too large, so it does not capture the steep sides of the droplet or the tip of the wetting ridge. Figure 3a shows the topography of the top of a droplet on a substrate with a stretch of $\epsilon = 50\%$. This is not completely spherical, as shown in Figure 3b, which gives the deviation of this data from a best-fit sphere. This has a saddle-shaped profile, consistent with a larger

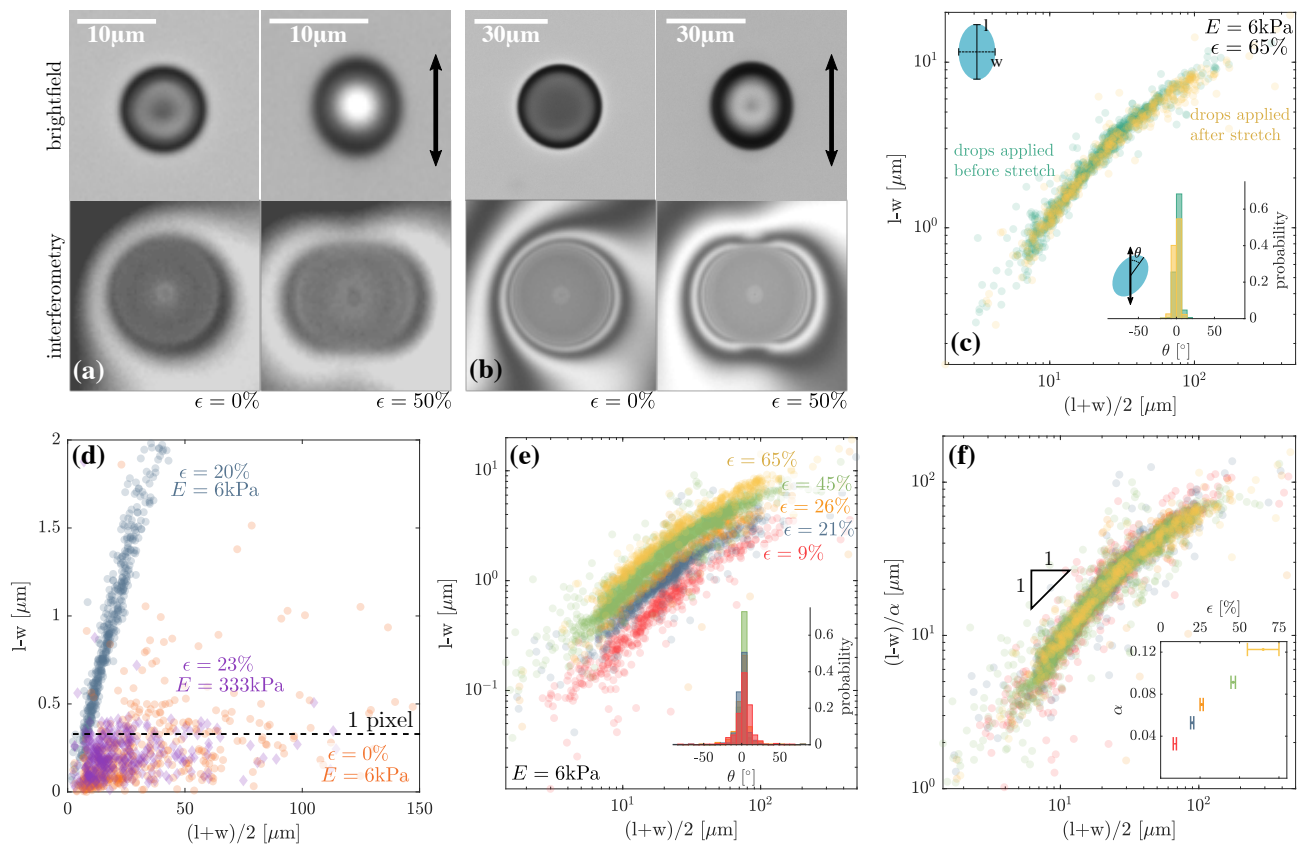


FIG. 2: Droplet shapes become elliptical on soft, stretched substrates. a,b) Brightfield (top) and interferometry (bottom) images for two droplets of different sizes, when the substrate is relaxed (left) and after 50% stretch (right). The stretch direction is indicated by the arrows. c) There is no observable contact line hysteresis for droplets. Droplets are the same shape regardless of whether they are applied to a soft, stretched substrate before it is stretched (green) or after (yellow). The inset histograms show the alignment of droplets with the stretch direction. d) Droplets are essentially round (to pixel resolution) on unstretched, soft silicone (red circles) and stretched, stiff silicone (purple diamonds). The blue data shows droplet shapes on soft silicone with a similar stretch for comparison. e) $l - w$ for glycerol droplets on soft silicone substrates increases with droplet size and stretch. The inset histograms show the alignment of droplets with the stretch direction. f) The data from e) collapses onto a single curve, when each data set is divided by the average slope, α , of the data for $(l + w)/2 < 20\mu\text{m}$. The inset shows this collapse parameter α as a function of ϵ .

radius of curvature, R_c in the stretch direction. Indeed, when we fit circles through the cap at different angles, ϕ , to the stretch direction and plot their radius (Figure 3c), we see that $R_c(\phi)$ is periodic and several microns larger when parallel to stretch than in the perpendicular direction. Thus, the droplet is ellipsoidal.

The ellipsoidal shape of the droplet is also consistent with its elliptical footprint. In Figure 3d, we plot the height profile data through the top of the droplet parallel and perpendicular to the stretch direction (green/purple data respectively). We also show the fitted circles with $R_{\parallel} = 59.7 \pm 0.6\mu\text{m}$ and $R_{\perp} = 55.7 \pm 0.6\mu\text{m}$. Taking $l = 2R_{\parallel}$ and $w = 2R_{\perp}$, gives a value of $l - w = 8.0\mu\text{m}$, which is close to the recorded ellipticities for similar sized droplets at comparable stretches in Figure 2e. Additionally, when we extrapolate the fitted circles from the top of the droplet towards the contact line, they match well with the substrate profile just outside the droplet, as shown in the inset to Figure 3d. The difference in radii of cur-

vature implies that there is a difference in the apparent contact angle parallel and perpendicular to the stretch directions. However, for the values here (and thus for most combinations of droplet size and stretch), this would be $\lesssim 2^\circ$ and thus too small to reliably detect with typical setups. Thus, it is not surprising that previous measurements of contact angles on larger droplets did not observe any dependence on substrate deformation [21, 23].

The classical theory of wetting for flat, uniform surfaces (*i.e.* Young-Dupr e) only depends on scalar surface energies. Even if the surface energy were strain-dependent, it would still predict circular contact lines. A clue to the missing physics is given in Figure 2f, where the transition away from a constant aspect-ratio regime always happens at the same lengthscale, independent of ϵ . This is the hallmark of an elastocapillary effect [24]. Elastocapillary phenomena are characterized by a shift in behavior around one of the elastocapillary lengths, Υ/E or γ_{lv}/E , where Υ is the solid's surface stress and γ_{lv} is

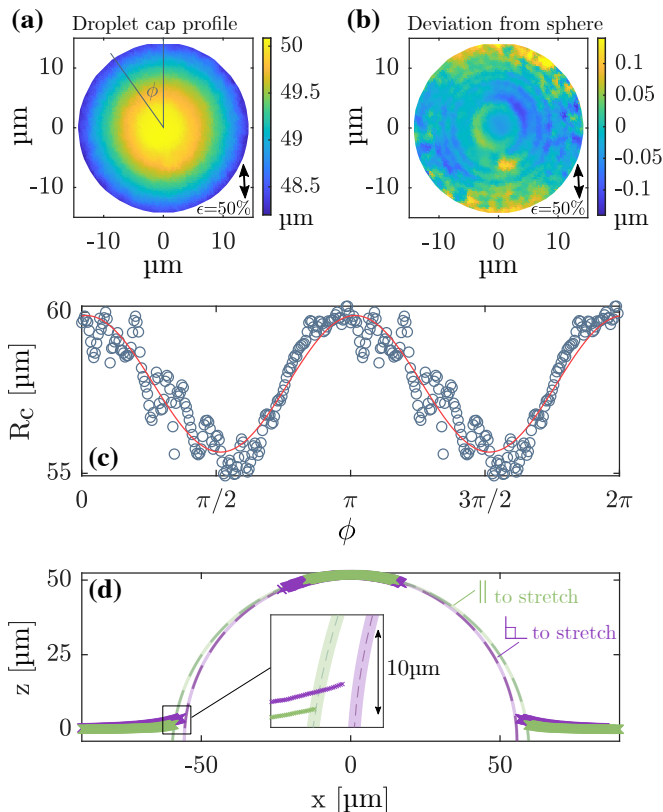


FIG. 3: White-light interferometry measurements show that droplets are not spherical. We measure the shape of a droplet on a substrate with a $50 \pm 10\%$ stretch. a) The top profile of the droplet. b) The same data after a best-fit spherical profile is subtracted gives a saddle shape. c) The radius of curvature, R_c , through the top of the droplet at different angles to the stretch direction. The red curve is a best fit to the data of a sinusoidal function with period π . d) Profiles through the droplet parallel (green) and perpendicular (purple) to the stretch direction. Dashed curves are fitted circles through the data at the top of the droplet. These fitted circles match with the contact line data (see inset), suggesting that they represent the droplet shape accurately. The shaded region around the fitted circles represent the uncertainty in the fits.

the droplet's surface tension (*e.g.* [24–28]). For our soft substrates, these lengthscales are $\mathcal{O}(10 \mu\text{m})$ [17]. Below this lengthscale, we generically expect surface properties to dominate behavior over bulk elasticity.

In the limit of small droplets, we therefore expect droplet shape to be determined by a balance between the surface stresses of the substrate, and the surface tension of the droplet. If the surface stresses are strain independent and thus isotropic, we would expect droplets to remain spherical. However, if surface stresses are strain-dependent, as reported in [23, 29], we would expect behavior like that of a droplet on a stretched, elastic membrane. In that case, droplets elongate and align with the stretch direction [14], as we see in the small-droplet limit of our experiments. In the limit of large droplets, much bigger than the elastocapillary lengthscale, we expect to

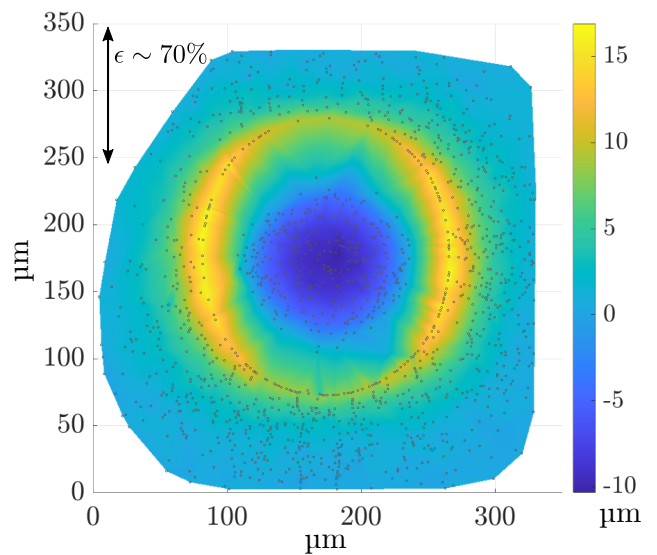


FIG. 4: The surface profile under a droplet on a stretched substrate is very asymmetric. We use confocal microscopy to measure the height profile of fluorescent nanobeads that are attached to the surface of the silicone gel under a glycerol droplet. Points indicate the measured bead positions, while the color is an interpolated surface profile. Here, $\epsilon \approx 70\%$.

recover the classical wetting behavior of Young-Dupré, and so droplet asymmetry should vanish. This is consistent with the lack of asymmetry of droplets on the stiffer substrate in Figure 2d, where the elastocapillary lengths are of order $\mathcal{O}(100 \text{ nm})$.

Elastocapillary effects revolve around substrate deformations. Thus, if droplet elongation is elastocapillary in origin, we expect anisotropic substrate deformations around the droplet. This is hinted at by the interferometry images in Figure 2a, but is properly visualized via confocal measurements of the surface profile under the droplet, as in Figure 4. This clearly shows the wetting ridge at the contact line and how it is significantly shorter in the direction of the applied $\epsilon \approx 70\%$ uniaxial stretch. A similar anisotropy of the wetting ridge was previously reported [23], and attributed to the presence of a strain-dependent surface stress of the substrate.

This ridge anisotropy likely underlies the asymmetric droplet shapes. Previous work has shown that the presence of a wetting ridge reduces the energy of a droplet, much like a negative line tension, predominantly by covering up droplet surface area [30]. Taller ridges lower the energy more, so a droplet will extend in the direction of stretch, as then a larger fraction of its contact line will feature a taller wetting ridge.

Wetting ridge anisotropy could also explain droplets' anisotropic motion. Previous studies of droplet sliding on soft substrates found that viscoelastic dissipation within the wetting ridge is rate limiting [31–34]. Simply stated, taller ridges dissipate more energy, so droplets travel

more slowly. Since we observe both faster droplet motion (Figure 1) and shorter wetting ridges (Figure 4) in the direction of applied stretch, we suspect that asymmetric viscoelastic dissipation underlies the observed differences in droplet speed.

In conclusion, we have shown that a simple, flat, soft, stretched substrates show asymmetric wetting, with a particularly strong effect on wetting dynamics. This is significant, as most asymmetrically-wetting substrates are significantly more complex. Substrate stretch could represent a novel approach to droplet control, that can be easily tuned *in situ*. Thus, it could modulate processes including adhesion [35], condensation [36], and coalescence [37], and drive movement along strain gradients (*c.f.* [38]).

Our observations cannot be explained with a classical, macroscopic description of wetting. Instead they are

elastocapillary phenomena, driven by microscopic, asymmetric deformations of the substrate under droplets. Despite recent progress in theory, there is still no consensus on how macroscopic stresses couple to elastocapillary deformations. One school of thought proposes that strain-dependent surface stresses play a vital role [23, 29, 39, 40]. Alternatively, recent work has proposed that nonlinear focusing of bulk stresses at contact lines control the deformations [41]. We hope that a theoretical analysis of these new experimental results will pinpoint the key physics.

Acknowledgments

This research was funded by the Swiss National Science Foundation (grant number 200021-172827).

-
- [1] A. R. Parker and C. R. Lawrence, *Nature* **414**, 33 (2001).
 [2] Y. Zheng, H. Bai, Z. Huang, X. Tian, F.-Q. Nie, Y. Zhao, J. Zhai, and L. Jiang, *Nature* **463**, 640 (2010).
 [3] Y. Zheng, X. Gao, and L. Jiang, *Soft Matter* **3**, 178 (2007).
 [4] D. Xia, L. M. Johnson, and G. P. López, *Adv. Materials* **24**, 1287 (2012).
 [5] T. Squires and S. Quake, *Rev. Mod. Phys.* **77**, 977 (2005).
 [6] M. Gleiche, L. Chi, E. Gedig, and H. Fuchs, *ChemPhysChem* **2**, 187 (2001).
 [7] M. Grsoy, M. T. Harris, A. Carletto, A. E. Yaprak, M. Karaman, and J. P. S. Badyal, *Colloids and Surfaces A: Physicochemical and Engineering Aspects* **529**, 959 (2017).
 [8] M. K. Chaudhury and G. M. Whitesides, *Science* **7256**, 1539 (1992).
 [9] M. Morita, T. Koga, H. Otsuka, and A. Takahara, *Langmuir* **21**, 911 (2005).
 [10] K.-H. Chu, R. Xiao, and E. N. Wang, *Nature materials* **9**, 413 (2010).
 [11] N. A. Malvadkar, M. J. Hancock, K. Sekeroglu, W. J. Dressick, and M. C. Demirel, *Nature materials* **9**, 1023 (2010).
 [12] H. Kusumaatmaja, R. Vrancken, C. Bastiaansen, and J. Yeomans, *Langmuir* **24**, 7299 (2008).
 [13] R. D. Schulman and K. Dalnoki-Veress, *Phys. Rev. Lett.* **115**, 206101 (2015).
 [14] R. D. Schulman, R. Ledesma-Alonso, T. Salez, E. Raphaël, and K. Dalnoki-Veress, *Phys. Rev. Lett.* **118**, 198002 (2017).
 [15] D. Kumar, T. P. Russell, B. Davidovitch, and N. Menon, *Nature materials* pp. 1–4 (2020).
 [16] R. Pericet-Camara, A. Best, H.-J. Butt, and E. Bonaccorso, *Langmuir* **24**, 10565 (2008).
 [17] R. W. Style, Y. Che, J. S. Wettlaufer, L. A. Wilen, and E. R. Dufresne, *Phys. Rev. Lett.* **110**, 066103 (2013).
 [18] A. Bardall, K. E. Daniels, and M. Shearer, *Eur. J. Appl. Math.* **29**, 281 (2018).
 [19] R. W. Style, Y. Che, S. J. Park, B. M. Weon, J. H. Je, C. Hyland, G. K. German, M. P. Power, L. A. Wilen, J. S. Wettlaufer, et al., *Proc. Nat. Acad. Sci.* **110**, 12541 (2013).
 [20] J. Y. Kim, Z. Liu, B. M. Weon, T. Cohen, C.-Y. Hui, E. R. Dufresne, and R. W. Style, *Science Advances* **6** (2020).
 [21] R. D. Schulman, M. Trejo, T. Salez, E. Raphaël, and K. Dalnoki-Veress, *Nature Commun.* **9**, 982 (2018).
 [22] R. W. Style, R. Boltanskiy, B. Allen, K. E. Jensen, H. P. Foote, J. S. Wettlaufer, and E. R. Dufresne, *Nature Phys.* **11**, 82 (2015).
 [23] Q. Xu, R. W. Style, and E. R. Dufresne, *Soft Matter* **14**, 916 (2018).
 [24] R. W. Style, A. Jagota, C.-Y. Hui, and E. R. Dufresne, *Ann. Rev. Condens. Matter Phys.* **8**, 99 (2017).
 [25] J. A. Zimmerman, N. Sanabria-DeLong, G. N. Tew, and A. J. Crosby, *Soft Matter* **3**, 763 (2007).
 [26] A. Jagota, D. Paretkar, and A. Ghatak, *Phys. Rev. E* **85**, 051602 (2012).
 [27] S. Mora, T. Phou, J.-M. Fromental, and Y. Pomeau, *Phys. Rev. Lett.* **113**, 178301 (2014).
 [28] A. Chakrabarti and M. K. Chaudhury, *Langmuir* **29**, 6926 (2013).
 [29] Q. Xu, K. E. Jensen, R. Boltanskiy, R. Sarfati, R. W. Style, and E. R. Dufresne, *Nature Commun.* **8**, 555 (2017).
 [30] L. A. Lubbers, J. H. Weijs, L. Botto, S. Das, B. Andreotti, and J. H. Snoeijer, *J. Fluid Mech.* **747**, R1 (2014).
 [31] A. Carre, J.-C. Gastel, and M. E. R. Shanahan, *Nature* **379**, 432 (1996).
 [32] S. Karpitschka, S. Das, M. van Gorcum, H. Perrin, B. Andreotti, and J. Snoeijer, *Nature Commun.* **6**, 7891 (2015).
 [33] T. Kajiya, A. Daerr, T. Narita, L. Royon, F. Lequeux, and L. Limat, *Soft Matter* **9**, 454 (2013).
 [34] M. Zhao, J. Dervaux, T. Narita, F. Lequeux, L. Limat, and M. Roché, *Proc. Nat. Acad. Sci.* **115**, 1748 (2018).
 [35] M. Butler, F. Box, T. Robert, and D. Vella, *Phys. Rev. Fluids* **4**, 033601 (2019).
 [36] M. Sokuler, G. K. Auernhammer, M. Roth, C. Liu, E. Bonaccorso, and H.-J. Butt, *Langmuir* **26**, 1544 (2010).
 [37] M. Chudak, J. S. Kwaks, J. H. Snoeijer, and A. A. Darhu-

- ber, *Soft Matter* **16**, 1866 (2020).
- [38] S. Márquez, G. Reig, M. Concha, and R. Soto, *Phys. Biol.* **16**, 066001 (2019).
- [39] A. Pandey, B. Andreotti, S. Karpitschka, G. van Zwi-eten, E. van Brummelen, and J. Snoeijer, arXiv preprint arXiv:2003.09823 (2020).
- [40] S. Heyden, N. Bain, Q. Xu, R. W. Style, and E. R. Dufresne, arXiv preprint arXiv:2007.05045 (2020).
- [41] R. Masurel, M. Roché, L. Limat, I. Ionescu, and J. Der-vaux, *Phys. Rev. Lett.* **122**, 248004 (2019).